# SPONTANEOUS RADIATION BACKGROUND CALCULATION FOR LCLS*

S. Reiche†, UCLA, Los Angeles, CA 90095-1547, USA


*Abstract*

The intensity of undulator radiation, not amplified by the FEL interaction, can be larger than the maximum FEL signal in the case of an X-ray FEL. In the commissioning of a SASE FEL it is essential to extract an amplified signal early to diagnose eventual misalignment of undulator modules or errors in the undulator field strength.

We developed a numerical code to calculate the radiation pattern at any position behind a multi-segmented undulator with arbitrary spacing and field profiles. The output can be run through numerical spatial and frequency filters to model the radiation beam transport and diagnostic.

In this presentation we estimate the expected background signal for the FEL diagnostic and at what point along the undulator the FEL signal can be separated from the background. We also discusses how much information on the undulator field and alignment can be obtained from the incoherent radiation signal itself.


## INTRODUCTION

Based on the successful demonstration of the Self-Amplified Spontaneous Radiation (SASE) Free-Electron Lasers (FEL) principle at longer wavelength [1, 2, 3], several X-ray FELs have been proposed and are currently under construction [4, 5]. The unique properties of the high-brightness radiation source allows to study femto-second processes with an Ångstrom spatial resolution, beneficial for all branches of sciences [6].

For SASE FELs the seeding field is the spontaneous radiation, although only a small bandwidth is amplified by the FEL process. The remaining part is emitted as a background signal, illuminating any detector to measure the FEL radiation. Because the total emitted power scales with the square of the energy of the driving electron beam [7], X-ray Free-electron lasers are more affected by the spontaneous radiation than FELs operating at longer wavelength. It is essential to estimate the spontaneous radiation due to three reason. First, the radiation power can be larger than the maximum FEL signal, yielding a large heat load on all X-ray optics elements. Second, the energy loss is strong enough to shift the electrons out of the FEL bandwidth, unless it is compensated by a taper of the undulator field. Third, spontaneous radiation overlaps with the FEL signal and defines the background signal for the FEL measurements.

* Work supported by the U.S. Department of Energy contract DE-AC02-76F00515

† reiche@physics.ucla.edu

From the FEL point of view it is essential to know the spectral and angular distribution of the spontaneous distribution to optimize the experimental set-up for the highest signal-noise ratio. Because the LCLS undulator lattice consists out of undulator modules and quadrupoles which are arrange with two short and one long drift sections between modules and because the closest detector is not place in the far field zone of the undulator, simple analytical calculations of the spontaneous radiation are not sufficient. For that reason we developed a numerical code to calculate the explicit background signal at the detector location. the algorithm is from first principle, based on the Lienard-Wichert potential [8]. The initial results for the LCLS undulator are presented here.

## ANALYTICAL MODEL

The total radiated power from the incoherent part of the undulator radiation is given by [7]

$$P = \frac{N_u}{6} Z_0 I e k_u \gamma^2 K^2 \quad , \tag{1}$$

where $N_u$ is the number of undulator periods, $Z_0 \approx 377\ \Omega$ is the vacuum impedance, $I$ the beam current, $e$ the electron charge, $k_u = 2\pi/\lambda_u$ the undulator wavenumber with $\lambda_u$ as the undulator period, $\gamma$ the electron energy in units of its rest mass energy, and $K$ the undulator parameter. For LCLS parameters the emitted power is 75 GW [5], about 10 times larger than the maximum FEL signal. Enhancement due to the coherent emission at longer wavelengths are negligible.

Eq. 1 allows to calculate the total energy loss, which is sufficient to derive the required taper of the undulator field in order to preserve the resonance condition. However it lacks any angular or spectral information. To calculate the radiation seen by a detector behind the undulator, the electric field is

$$\vec{E} = \frac{e}{4\pi\epsilon_0 c} \frac{\vec{n} \times [(\vec{n} - \vec{\beta}) \times \dot{\vec{\beta}}]}{(1 - \vec{n}\vec{\beta})^3 R} \quad , \tag{2}$$

evaluated at the retarded time. Neither the direction of observation $\vec{n}$ nor the distance $R$ between source and target is constant for LCLS FEL , where the closest detector is located 113 m behind the exit of the 130 m long, multi-segment undulator.

The emission is the strongest due to the maximum Doppler shift, where the electron moves parallel to the direction of observation, fulfilling the condition

$$\frac{K}{\gamma} \sin(k_u z) = \frac{n_x}{n_z} \quad . \tag{3}$$

Eq. 3 is only valid for observation angles $\theta$ between 0 and $K/\gamma$ in the $xz$-plane. Beyond that as well as in the $yz$-plane the radiation intensity drops like the normal synchrotron radiation with a characteristic fall-off of $1/\gamma$. Note that the signal from a single period is antisymmetric in the retarded time frame with respect to the emission time at $z = \lambda/2$. The forward direction shows alternating, equally spaced unipolar pulses. The pulses are narrow due to the Doppler effect and excite a rich harmonic content of odd harmonics. To estimate the number of harmonics, we calculate the pulse length in the retarded time frame. The pulse shape is dominated by the denominator in Eq. 2 and scales as $E \propto (1-\beta_z)^{-2}$. With $\beta_z = 1 - (1 + K^2/2)/2\gamma^2 + (K^2/4\gamma^2)\cos(2ck_u t)$ the full-width half maximum is given by

$$\Delta T = \frac{1}{ck_u}\cos^{-1}\left[\frac{2(1-\sqrt{2})+K^2}{K^2}\right] \quad .$$

In the retarded time frame it becomes

$$\Delta\tau = \frac{1+K^2/2}{2\gamma^2}\Delta T - \frac{K^2}{4ck_u\gamma^2}\sin(ck_u\Delta T) \quad .$$

The ratio between resonant wavelength and FWHM of the observed pulse length ($c\Delta\tau$) defines the harmonic content. For LCLS parameters the value is 120.

For larger observation angles in the $xz$-plane pairs of adjacent unipolar pulses are shifted closer to each other till they merge to a single bipolar pulse at an angle of $\theta = K/\gamma$ and beyond. The emission of each $n$th harmonic has $n-1$ knots in the $xy$-plane and is slightly more confined in the forward direction than the fundamental, because the observed pulses are wider due to the reduced curvature in the electron trajectory, where Eq. 3 is fulfilled.

## NUMERICAL MODEL

The program SPUR (SPontaneous Undulator Radiation) has been written to calculated the radiation pattern from an arbitrary undulator lattice at any point behind the undulator. It supports parallel architecture with a master-slave configuration using the Massage Passing Interface (MPI) method [9], where a master node assigns the work to slave nodes and thus optimizes the CPU usage for asymmetric nodes or unbalanced load upon a symmetric cluster.

Either the radiation pattern from a single electron onto a two dimensional grid or from multiple electrons onto a single point in space can be calculated, including single electron to single point configuration. The program is based on Eq. 2, calculating the time-domain signal in the retarded time frame. Fourier transformation methods of uneven sampled data [10] have shown an unacceptable level of noise, compared to standard Fast Fourier Transformation (FFT) of the signal, after it has been interpolated to an equidistant grid.

The undulator lattice can be defined down to each individual pole, including arbitrarily long drift sections between undulator modules. The electron trajectory is analytical calculated for each undulator period with a step width, sufficiently small enough to resolve all harmonics. In the case for LCLS with more than 100 harmonics, at least 256 steps per period are required and then interpolated to a 4 times finer grid in the retarded time frame to achieve convergence in the spectrum. For LCLS with a total of about 3700 periods it yields record sizes for the FFT of about 7 million sample points. Thus the memory demand is limited to 100 MByte. To reduce the output for runs with a large number of grid points, the spectrum can be downsampled to a frequency resolution, lower than the maximum resolution $\Delta f/(\lambda/c) \approx 1/N_u$.

## RADIATION PROPERTIES

At LCLS the first detector station is located 113 m behind the end of the undulator [4]. It is exposed to the highest intensity of both FEL and spontaneous radiation compared to the second diagnostic station, which is further downstream of the X-ray beam transport line. Due to the close proximity of the first detector to the undulator, the calculation of the radiation cannot be simplified by assuming the far field zone. First, the $R^{-2}$-dependence of the emission sources along the undulator with respect to the fixed detector location is noticible. Second, the angle of observation is not constant for off-axis position, but shifts towards larger values. As a consequence a systematic redshift dominates the width of the harmonics, which minimal value of $1/N_u$ can only be observed on-axis. While the intrinsic energy spread is smaller than $1/N_u$, the finite beam size and divergence has a non-negligible effect on the bandwidth as well.

At the detector location the peak intensity is 20 GW/cm$^2$, illuminating an area of $6\times 2$ cm$^2$ (full width in the $x$- and $y$-direction). The observed total power is 75 GW, which has a contribution of 0.6 GW due to the coherent emission of the bunch profile [11]. Fig. 1 shows the intensity distribution at the first detector location.

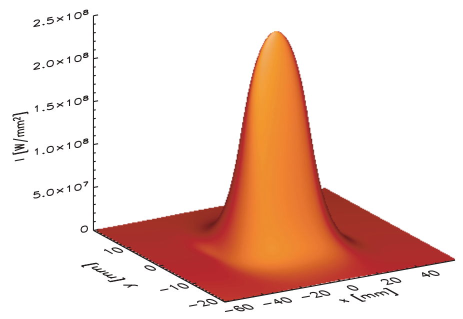


Figure 1: Intensity distribution of the spontaneous radiation at the detector location, 113 m behind the LCLS undulator.

It is essential for the FEL amplification that all undulator modules are well tuned and aligned to the undulator axis. The on-axis field requirement is $\Delta K/K \approx 10^{-4}$ [5], which would be desirable to measure it for each undulator module individually. However this information cannot be extracted from the radiation distribution and intensity, which are insensitive to such small variation. The most promising measurement is the width of the harmonics of the on-axis radiation. While the fundamental harmonic has an intrinsic width of about 1% – corresponding to 112 undulator periods per module – a change in the width on a percent level is difficult to measure, but the effect of a detuned module becomes enhanced with higher harmonics. E.g. at the 100th harmonics the shift in the wavelength due to a detuning of $\Delta K/K \approx 10^{-4}$ is 1% and thus comparable to the intrinsic bandwidth. However the width can be broaden by beam trajectory alignment and the beam emittance and thus obscure the measurement. It seems more beneficial to derive the undulator field quality from the power versus undulator position measurement of the FEL signal.

## BACKGROUND SIGNAL FOR THE FEL RADIATION

The radiation power of the incoherent emission is about 75 GW and therefore 10 times larger than the expected saturation power level of the FEL at 1.5 Ångstroem. To improve the signal to noise ratio the incoherent background signal can be either cut by spatial aperture limitation or by bandpass filters. In this section we estimate the efficiency of both methods. It excludes the frequency dependent sensitivity of the X-ray detector, which are typically less efficient at higher frequencies than at the FEL frequency [12]. The estimate, given below, is an upper limit for the detected signal.

Time-dependent FEL codes, such as Ginger or Genesis 1.3, cannot predict the total background signal, because they model only a narrow bandwidth around the resonant wavelength for an optimized calculation of the FEL process [13]. The typical full bandwidth in the FEL simulation of X-ray lasers such as LCLS and TESLA is between 5% and 10%. In addition the code discretize the radiation field to a finite set of radiation modes, imposing a limit on the maximum angle of emission. These cuts do not affect the result of the FEL simulation because strongly diffracting modes as well frequency deviation larger than the FEL bandwidth are amplified by the FEL process. To add the correct background signal, the spontaneous signal from the FEL simulation is removed first by subtracting the linear trend in the start-up process of the FEL signal. Then the background signal, calculate by SPUR, is added.

The FEL signal is much more confined in the spatial direction than the spontaneous radiation. With an rms diffraction angle of about 1 $\mu$rad the FEL signal covers an area of about 3 mm$^2$ at the detector position 113 m behind the end of the LCLS undulator. A smaller aperture would cut the FEL signal, which is not in the interest of the measurement. In the contrary the aperture has to be larger to allow for jitter in the FEL beam centroid. The dependence of the

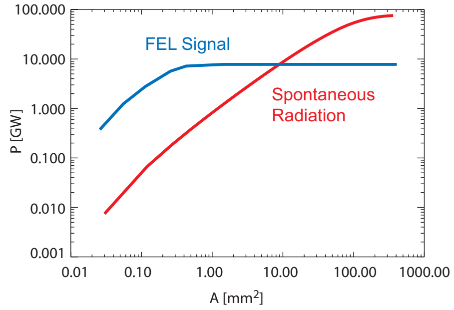


Figure 2: Detected power of the FEL signal and the spontaneous radiation for an aperture limit at the detector location, 113 m behind the undulator exit.

spontaneous radiation background signal and the FEL signal on the aperture is shown in Fig. 2. With an aperture of 1 mm$^2$ 0.9 GW of the spontaneous radiation is detected, resulting in a signal-to-noise ratio of only 10:1. If the detector is array-based like a CCD camera, the measurement is rather intensity than power based. In case for LCLS the ratio between the intensities is 100 to 1, an improvement of one order of magnitude compared to a collecting detector with the aperture of 1 mm$^2$, mentioned above.

Spatial cuts are inferior to spectral cuts because even under the best circumstances a spatial aperture cannot filter out higher harmonics. For high $K$ undulator such as LCLS a large number of odd harmonics are emitted on-axis, some of them with higher power than the fundamental. A significant reduction can be achieved when only the emission at the resonant wavelength is collected. Although higher harmonics can contribute to the resonant wavelength due to the red shift for larger emission angles $\theta$, they can be filtered out by a loose spatial cut. For the second harmonic the angle to shift the wavelength to the fundamental wavelength is 100 $\mu$rad and can be easily collimated by a 1 cm$^2$ aperture in front of the LCLS detector.

Due to the intrinsic width of $\delta f/f_0 = 1/N_u$ of the spontaneous signal the radiation at the resonant wavelength is confined in the opening angle of

$$\Delta\theta = \frac{K}{2\gamma}\sqrt{\frac{1}{N_u}},$$

with $\Delta\theta = 1.5$ $\mu$rad for LCLS parameters. This correspond to an emission of 1 MW per 0.1% bandwidth. The full FEL signal falls within this bandwidth, yielding a signal-to-noise ratio of about $10^4$:1. Even wider bandwidth cuts are still superior to the spatial collimation. The detectable FEL signal for LCLS and various methods of reducing the spontaneous background is shown in Fig. 3

From the point of view of detecting the FEL signal the situation is improved when the FEL is operated at lower energy, because the saturation power has a weak dependence on the energy while the incoherent radiation is 10 times smaller for a FEL wavelength of 1.5 nm. In addition the

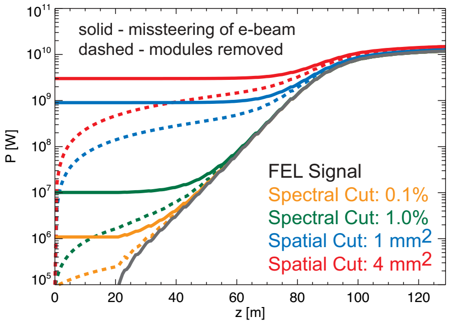


Figure 3: Detectable FEL signal for various method to reduce the background signal of the spontaneous radiation.

Table 1: Power level of the LCLS FEL and background signal for various spatial and spectral cuts at the near hall detector.

| Signal | 1.5 Å | 1.5 nm |
|---|---|---|
| FEL | 8 GW | 4 GW |
| Spontaneous Radiation | 75 GW | 7.5 GW |
| Spectral Cut: 0.1% | 1 MW | 100 kW |
| Spectral Cut: 1.0% | 10 MW | 1 MW |
| Spatial Cut: 1 mm$^2$ | 0.9 GW | 9 MW |
| Spatial Cut: 4 mm$^2$ | 3 GW | 30 MW |

opening angle is increased by $\sqrt{10}$, so that the on-axis intensity drops by two orders of magnitude for spatial cuts. Because the coherence angle is also increased the spectral power in a narrow bandwidth is improved only by a factor of 10. Tab. 1 summarize the different power levels of the FEL and background signal for the two limits in the FEL wavelength of LCLS.

## CONCLUSION

We have written a numerical code to calculated the background signal from the spontaneous radiation at a given location to detect the X-ray FEL signal. Due to the complex lattice of the undulator and the close proximity of the detector the spontaneous radiation can be estimated analytically only in crude approximation and detailed numerical calculations are required. With a given intensity distribution and the associated spectrum of the background signal the X-ray optics and detector can be optimized to maximize the signal to noise ratio of the FEL signal.

Because the on-axis spectrum is rich in harmonics, spatial collimation are less efficient than spectral filters (monochromators or dispersive optical elements). In the ideal case, when only 0.1% of the spontaneous radiation illuminates the detector the background signal is dropped to 1 MW, while the FEL signal is not affected. Detection of the FEL signal after 20 m of undulator becomes possible. All modules after that point can be examine by the exponential growth for optimum alignment and tuning.

## REFERENCES

[1] A. Tremaine *et al.*, Phys. Rev. Lett. **88** (2002) 204801

[2] S.V. Milton *et al.*, Science **292** (2001) 2037

[3] V. Ayvazyan *et al.*, Phys. Ref. Lett. **88** (2002) 104802

[4] *Linac Coherent Light Source (LCLS)*, SLAC-R-521, UC-414 (1998)

[5] TESLA-FEL 2001-05, Deutsches Elektronen Synchrotron, Hamburg, Germany (2001)

[6] C. Pellegrini and J. Stöhr, Nucl. Inst. & Meth. **A500** (2003) 33

[7] K.J. Kim, in AIP Conference Proceedings **184**, M. Month and M. Dienes, eds., (1989) 585

[8] J.D. Jackson, *Classical Electrodynamics*, (John Wiley and SOns, New York, 1975)

[9] Message Passing Interface Forum, Computer Science Dept. Techincal Report CS-94-230, University of Tennessee, Knoxville (1994)

[10] N.R. Lomb, Astrophysics and Space Science **39** (1976) 447

[11] S. Reiche and Z. Huang,*Coherent Radiation Effects in the LCLS Undulator*, presented at this conference.

[12] R. Bionta, *private communication*

[13] Z. Huang and K.-J. Kim, Nucl. Inst. & Meth. **A507** (2003) 65